

## Article

# A Design and Optimization of a CGK-Based Fuzzy Granular Model Based on the Generation of Rational Information Granules

Chan-Uk Yeom<sup>1</sup> and Keun-Chang Kwak<sup>1,2,\*</sup> 

<sup>1</sup> Center for IT-Bio Convergence System Agriculture, Chonnam University, Gwangju 61186, Korea; walt18@naver.com

<sup>2</sup> Department of Electronics Engineering IT-Bio Convergence System, Chosun University, Gwangju 61452, Korea

\* Correspondence: kwak@chosun.ac.kr; Tel.: +82-062-230-6086

**Abstract:** This study proposes an optimized context-based Gustafson Kessel (CGK)-based fuzzy granular model based on the generation of rational information granules and an optimized CGK-based fuzzy granular model with the aggregated structure. The conventional context-based fuzzy-c-means (CFCM) clustering generates clusters considering the input and output spaces. However, the prediction performance decreases when the specific data points with geometric features are used. The CGK clustering solves the above situation by generating valid clusters considering the geometric attributes of data in input and output spaces with the aid of the Mahalanobis distance. However, it is necessary to generate rational information granules (IGs) because there is a significant change in performance according to the context generated in the output space and the shape, size, and several clusters generated in the input space. As a result, the rational IGs are obtained by considering the relationship between the coverage and specificity of IG using the genetic algorithm (GA). Thus, the optimized CGK-based fuzzy granular models with the aggregated structure are designed based on rational IGs. The prediction performance was compared using the two databases to verify the validity of the proposed method. Finally, the experiments revealed that the performance of the proposed method is higher than that of the previous model.

**Keywords:** CGK clustering; information granules; granular model; aggregated structure; optimization



**Citation:** Yeom, C.-U.; Kwak, K.-C. A Design and Optimization of a CGK-Based Fuzzy Granular Model Based on the Generation of Rational Information Granules. *Appl. Sci.* **2022**, *12*, 7226. <https://doi.org/10.3390/app12147226>

Academic Editors: Cheng-Jian Lin and Tsang-Chuan Chang

Received: 22 May 2022

Accepted: 14 July 2022

Published: 18 July 2022

**Publisher's Note:** MDPI stays neutral with regard to jurisdictional claims in published maps and institutional affiliations.



**Copyright:** © 2022 by the authors. Licensee MDPI, Basel, Switzerland. This article is an open access article distributed under the terms and conditions of the Creative Commons Attribution (CC BY) license (<https://creativecommons.org/licenses/by/4.0/>).

## 1. Introduction

A fuzzy set means a set in which each element has a degree of membership for a set. Studies on methodologies, algorithms, and structures are being conducted in various fields of application in the real world based on the fuzzy set [1–3]. Real-world problems with complex nonlinear characteristics need a hybrid intelligent model that has integrated the theories, structures, and technologies of various models. Integrating various computational techniques has an advantage over individual models for designing hybrid intelligent systems. A representative method that is frequently used with the hybrid intelligent system is the neuro-fuzzy reasoning system. The neuro-fuzzy inference system is a combined system that complements the shortcomings of the two models as a model that combines the parallel computation and learning capabilities of artificial neural networks and the human knowledge expression and explanation capabilities of the fuzzy system [4–8].

On the other hand, granular computing (GrC) is a computing paradigm that is newly emerging in the information processing field. GrC is a computational theory about using information granules (IGs) such as clusters, subsets, sections, groups, and classes for effective computation model design using information and knowledge about real-world applications [9–13]. Research related to GrC is being conducted in various fields, including information hiding in programming, granularity in artificial intelligence, divide and conquer algorithms in computational science, section computing, cluster analysis, fuzzy

and rough set theory, and database. Here, using the established concept of IGs formed in the fuzzy and rough set theory helps solve problems that arise in real-world applications. Pedrycz [14] proposed a granular model (GM) that represents the model output as a fuzzy number in the form of a triangle, instead of a numerical value, based on GrC. GM generates IGs using the Context-based Fuzzy C-Means (CFCM) clustering that applies the conventional FCM clustering. The CFCM clustering generates clusters by considering data characteristics in an output space and the input space. Studies on GM are being actively conducted now [15–20]. An analysis of the above-mentioned research trends indicates the need for research on methodology and optimization to generate rational IGs because the performance varies significantly according to the shape, size, and number of IGs.

Optimization, which is a process of finding solutions closest to the correct answer under certain constraints, is widely used in service management, product development, etc. Optimization algorithms are classified into global and local optimization techniques according to the required solution level. The global optimization technique [21] aims at finding the best solution in the entire search area even though it takes time to process, whereas the local optimization technique [22] aims at finding the best solution in a partial search area within a short time. There are various methodologies for optimization techniques, and the representative methods are genetic algorithm (GA) and particle swarm optimization (PSO). GA is a computational model using Darwin's theory of survival of the fittest, which explains the evolution of the biological system and a global optimization technique developed by Holland [23]. After expressing the problem to be solved by GA as data structures of a given format, and then they are gradually transformed to produce progressively better solutions. The PSO algorithm is an iterative optimization algorithm that attempts at social behavior simulation developed by Eberhart and Kennedy [24]. It started from the movements of entities that live in groups, such as ants, fish, and birds. Optimization is performed by converting the characteristic of these entities that move in groups when sharing information among them into a simple mathematical formula (GA [25–29], PSO [30–34]).

This study generates rational IGs using GA and performs the design and optimization of the context-based Gustafson Kessel (CGK)-based fuzzy granular model based on them. Context-based FCM clustering generates clusters by considering the characteristics of the data in input and output spaces, but it is difficult to process data with geometric features because it only generates circular clusters. To solve this problem, we propose context-based GK clustering that considers the geometric attributes of data in input and output spaces. When IGs are generated using the proposed context-based GK clustering, rational IGs are generated by balancing the coverage and specificity of the IGs. The performance of GM is improved by optimizing the number of IGs generated in input and output spaces using GA among optimization techniques to design and optimize the CGK-based fuzzy granular model based on rational IGs.

This paper is organized in the following order. Section 2 describes the context-based GK clustering and CGK-based fuzzy granular model. Section 3 explains the optimized CGK-based fuzzy granular model through IG assignment. Section 4 analyzes the experimental results and performance. Finally, Section 5 presents the conclusions and future research plans.

## 2. Design of the CGK-Based Fuzzy Granular Model

### 2.1. Context-Based GK Clustering

Clustering [35] is a method of data mining by defining a data group (cluster) in consideration of the characteristics of the given data and finding representative points of the data group. GK clustering [36] is a method of generating clusters considering the geometric attributes of data. However, it has the problem that only the data characteristics in the output space can be reflected because it only considers the data characteristics in the input space. Context-based GK clustering generates clusters by considering data characteristics in the output space. Figure 1 describes the concept of context-based GK clustering.

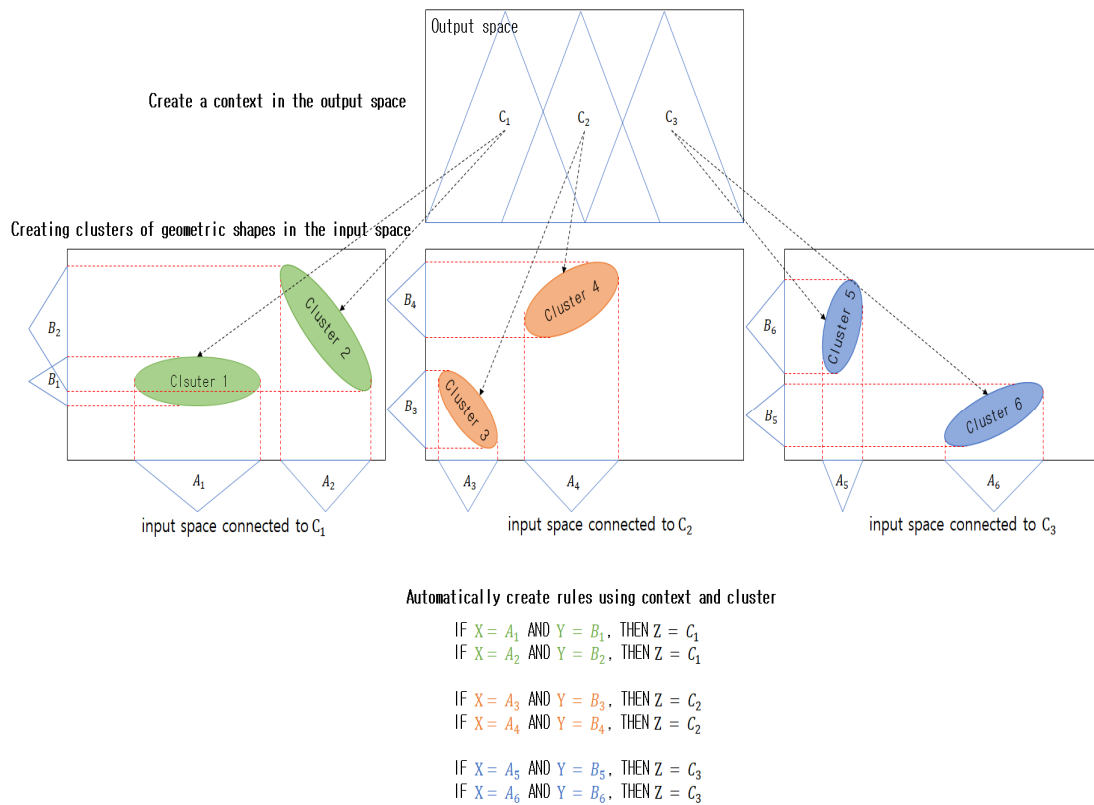


**Figure 1.** Concept of context-based GK clustering.

The context generated in the output space can be expressed as follows:

$$D : T \rightarrow [0, 1] \tag{1}$$

where  $D$  denotes the data in the output space. Assuming that there is a context generated considering the characteristics of data in the output space,  $f_k = T(d_k)$  expresses the degree of the context belonging to the  $k$ th data.

GK clustering generates clusters by using Equation (2) for the Mahalanobis distance between the centroid of the cluster and random data:

$$d_{GK}^2(x_k - v_i) = \|x_k - v_i\|_{A_i}^2 = (x_k - v_i)^T A_i (x_k - v_i) \tag{2}$$

where  $A_i$  denotes the matrix that has the fixed constant  $\det(A_i) = \rho_i$  for each  $i$ . GK clustering can consider even the data in the local part by expanding the concept of FCM clustering by using  $d_{GK}^2(x_k, v_i)$  so that various clusters of geometric shapes can be generated. The objective functions of GK clustering are expressed as Equations (3)–(5):

$$J_m^{GK}(\mu, v) = \sum_{k=1}^n \sum_{i=1}^c \mu_{ik}^m d_{GK}^2(X_k, v_i) \tag{3}$$

$$v_i = \frac{\sum_{k=1}^n \mu_{ik}^m x_k}{\sum_{k=1}^n \mu_{ik}^m} \tag{4}$$

$$\mu_{ik} = \frac{\|x_k - v_i\|_{A_j}^{-\frac{2}{m-1}}}{\sum_{j=1}^c \|x_k - v_j\|_{A_j}^{-\frac{2}{m-1}}} \tag{5}$$

Various clusters of geometric shapes are created in each context generated in the output space by repeating Equations (3)–(5).

- [Step 1] The number of contexts to be generated in the output space and the number of clusters to be generated in each context are selected, and then the degree of the geometric shape  $\varepsilon$  is selected, which  $\varepsilon$  must be larger than zero. The membership matrix  $U$  is initialized to a value between 0 and 1.
- [Step 2] A method of generating context in the output space is selected between two methods: uniformly generating contexts with a constant size; and flexibly generating in different sizes based on the Gaussian probability distribution. Contexts are generated by selecting one of these two methods.
- [Step 3] The centroid and membership matrix of the cluster is calculated in each context using Equation (4).
- [Step 4] The objective function of context-based GK clustering is calculated using Equations (3) and (6). The above process is repeated if the estimated value is larger than the previous value, and the above procedure is stopped if the calculated value is smaller than the last value.

$$\|\mu^t - \mu^{t-1}\| \leq \varepsilon \tag{6}$$

### 2.2. Context-Based GK (CGK) Fuzzy Granular Model

The CGK-based fuzzy granular model is designed by generating contexts using context-based GK clustering and then developing clusters of geometric shapes in each context. Figure 2 illustrates the structure of the CGK-based fuzzy granular model that generates three contexts and nine clusters. This figure shows there are the premise and conclusion variables. First, the conclusion variable is an IG of the context shape generated in the output space. Next, the premise variable is an IG of the cluster type generated in each context. The final output of the CGK-based fuzzy granular model is expressed as follows:

$$Y = \sum_{\oplus} W_t \otimes z_t \tag{7}$$

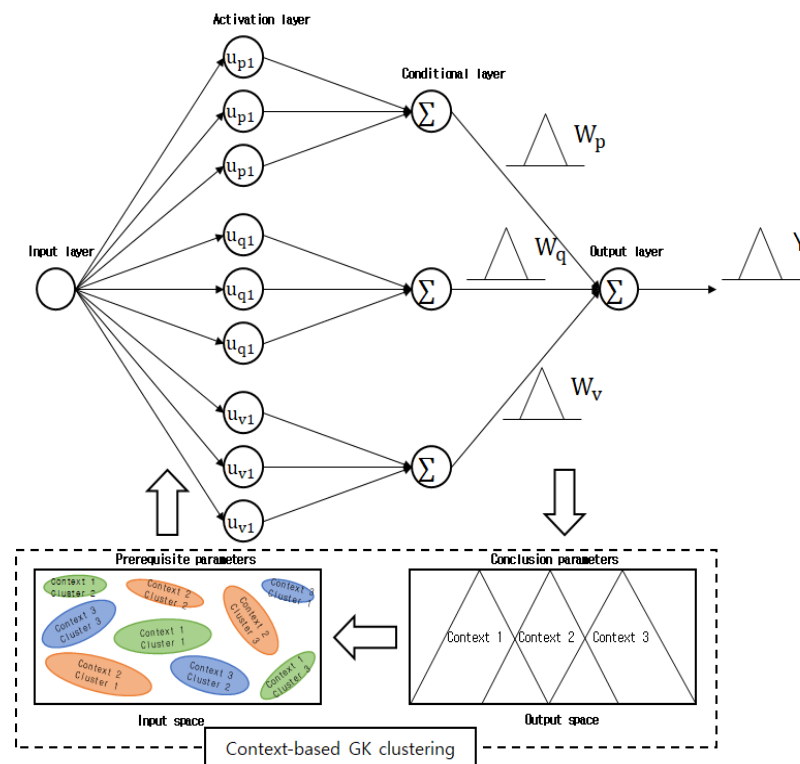


Figure 2. Structure of CGK-based fuzzy granular model.

In Equation (7),  $\oplus, \otimes$  are addition and multiplication signs that express the operations for IG. The fuzzy set is generated by processing the premise part of the CGK-based fuzzy granular model. The clusters generated by context-based GK clustering are expressed as an activation layer of the CGK-based fuzzy granular model. The part between the conditional and output layers is expressed as a linguistically descriptive context. The sum of final outputs of the CGK-based fuzzy granular model is expressed as follows using every context in the output space:

$$Y = (z_{11} \otimes A_1 \oplus z_{12} \otimes A_1 \dots z_{1n1} \otimes A_1) \oplus (z_{21} \otimes A_2 \oplus z_{22} \otimes A_2 \dots z_{2n2} \otimes A_2) \dots (z_{c1} \otimes A_c \oplus z_{c2} \otimes A_c \dots z_{cnc} \otimes A_c) \tag{8}$$

The final output of the CGK-based fuzzy granular model is expressed as a fuzzy number with the context shape and as a fuzzy set as follows:

$$Y_i = (y_i^-, y_i, y_i^+) \tag{9}$$

where  $y_i^-, y_i,$  and  $y_i^+$  are the lower limit, model value, and upper limit of the CGK-based fuzzy granular model, respectively. These values are expressed as Equations (10)–(12):

$$y_i^- = (z_{11}a_1 + z_{12}a_1^- + \dots + z_{1n1}a_1^-) + (z_{c1}a_c^- + z_{c2}a_c^- + \dots + z_{cnc}a_c^-) \tag{10}$$

$$y_i = (z_{11}a_1 + z_{12}a_1 + \dots + z_{1n1}a_1) + (z_{c1}a_c + z_{c2}a_c + \dots + z_{cnc}a_c) \tag{11}$$

$$y_i^+ = (z_{11}a_1 + z_{12}a_1^+ + \dots + z_{1n1}a_1^+) + (z_{c1}a_c^+ + z_{c2}a_c^+ + \dots + z_{cnc}a_c^+) \tag{12}$$

When context-based GK clustering is performed, the membership matrix is expressed as a value between 0 and 1. The requirements of the membership matrix are expressed as follows:

$$U(f) = \mu_{ik} \in [0, 1] \left| \sum_{i=1}^c \mu_{ik} = f_k \forall k \text{ and } 0 < \sum_{k=1}^N \mu_{ik} < N \tag{13}$$

The structural description of the CGK-based fuzzy granular model is as follows. The input layer receives data and passes them to the next layer. The activation layer is a process of generating clusters in the input space corresponding to contexts and a step for generating clusters of geometric shapes. For the premise layer, conditional clustering is performed in each context. The activation and premise layers are interconnected. Clusters are generated using context-based GK clustering when the contexts of the output space are given. In each context, as many clusters as selected are created, and the number of nodes summed in each output layer is similar to the number of contexts. The final output summed in the output layer is expressed as a context.

### 2.3. CGK-Based Fuzzy Granular Model with the Aggregated Structure

When extensive multivariate data are processed through a neuro-fuzzy reasoning system and GM, the number of rules increases exponentially as many input variables influence it. The calculation speed and performance of the neuro-fuzzy reasoning system and GM are decreased. A model that is connected hierarchically with two or more systems rather than a single neuro-fuzzy reasoning system or a single GM can be designed to address this problem. This study proposes the CGK-based fuzzy granular model of the aggregated structure that combines the CGK-based fuzzy granular model with the linear regression [37], artificial neural network [38], and radial basis function neural network [39]. The proposed model is constructed of an aggregated structure and uses linear regression, ANN, and a radial basis function neural network as sub-models and the CGK-based fuzzy granular model as an upper model to calculate the final output. The CGK-based fuzzy granular model of the aggregated structure can be designed more efficiently and easily understood than a single system and model when processing data with the same number of input variables [40,41].

The CGK-based fuzzy granular model of the aggregated structure uses the input variables of the original data as input for the linear regression, artificial neural network, and radial basis function neural network. It uses the model's output after the data are processed in each sub-model as input for the CGK-based fuzzy granular model, which is the upper model. Linear regression analyzes the correlation between input and output variables and is expressed as follows:

$$y_i = \beta_1 x_{i1} + \beta_p x_{ip} + \varepsilon_i = x_i^T \beta + \varepsilon_i, \quad i = 1, 2, \dots, n \tag{14}$$

In Equation (14), the parameter of linear regression is expressed as  $p$ , and the coefficient of each independent variable is expressed as  $\beta_i$ .  $x_i^T \beta$  expresses the inner product of  $x_i$  and  $\beta$ , and  $T$  denotes transposition. Lastly,  $\varepsilon_i$  is an error term and denotes an error variable that indicates the error between independent and dependent variables. The creation of ANN was inspired by the form of synaptic connection, and the model can solve problems by changing the connection strength through training. The general artificial neural network comprises three layers, the input, hidden, and output layers, respectively. The input layer passes the input variables of data to the hidden layer, and the number of input layers is the same as the number of input variables of the data to be processed. The mathematical calculation does not happen in the input layer, and it only plays the role of passing data. The hidden layer is composed of one or more layers. If there are two or more hidden layers, it is called a multilayer ANN. The output layer calculates the final output of the ANN and is processed by the activation function. The radial basis function neural network uses the activation function as a radial basis function of the structure mentioned above of ANN. Unlike the structure of general ANN, the radial basis function neural network only has one hidden layer. The weight can be effectively calculated because there is only one hidden layer. Figure 3 illustrates the CGK-based fuzzy granular model of the aggregated structure.

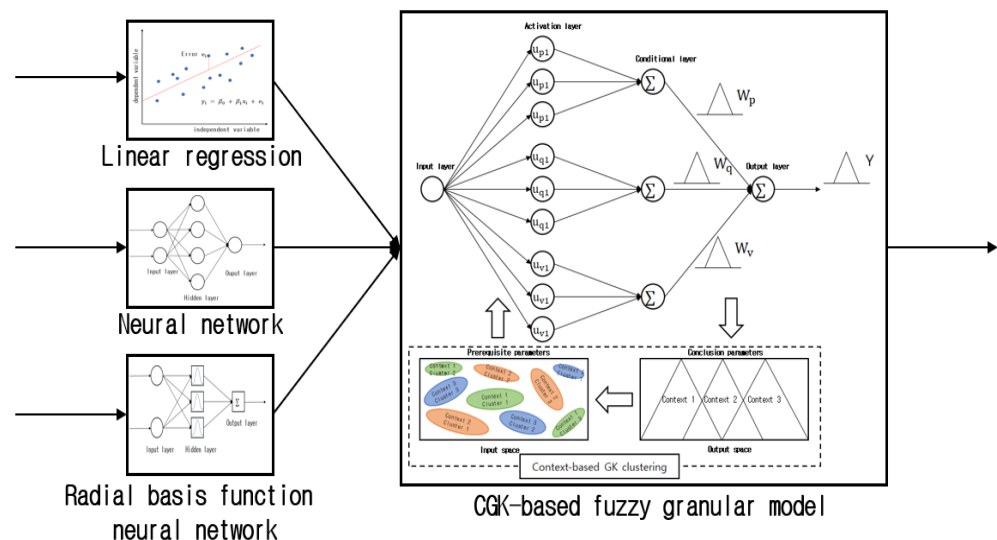


Figure 3. CGK-based fuzzy granular model of the aggregated structure.

The outputs from the sub-models, i.e., linear regression, artificial neural network, and radial basis function neural network, are combined and used as the input of the upper model, the CGK-based fuzzy granular model. The upper model, the CGK-based fuzzy granular model, generates IGs by selecting the number of contexts and the number of clusters and calculates the final output using them. The conventional GM had the problem of difficulty generating rational IGs when processing extensive multivariate data, and it took much time to process them. However, the fuzzy granular model of the aggregated structure proposed in this study can generate rational IGs from large multivariate data because they combine and use the outputs from sub-models as the input of the upper model.

### 3. Design of the Optimized CGK-Based Fuzzy Granular Model of the Aggregated Structure through IG Assignment

#### 3.1. Optimal Assignment of IGs

IGs are generated using clustering of original numerical data, and the GM is designed using the generated IGs. The following conditions should be satisfied when designing the GM. First, the data in the output space are granulated. Second, the data in the input space corresponding to each IG generated in the output space are granulated. The cluster's centroid generated through clustering in the input space is granulated. The considerations when designing the GM are as follows. The IG generation method is provided so that the model is granulated, and the IG is limited to the form specified by the user. The higher the value of the IG, the greater the design flexibility becomes. If the IG is 0, it is not granulated, and the model has the original numerical value. There are two general methods to generate IGs through information granulation described above: uniform and flexible generation methods. Figure 4 shows the original data conversion to IG through the information granulation method.

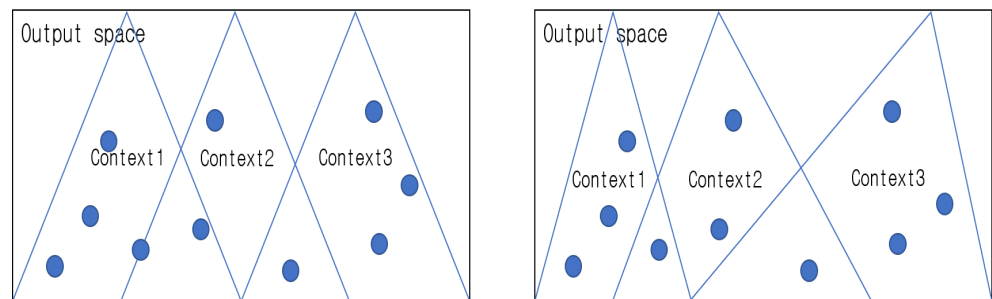


Figure 4. Shape of IGs generated through the information granulation method.

The uniform generation method generates the data in the output space symmetrically and uniformly under the level of information granulation, and  $N$  IGs show the same form. In Equations (15) and (16),  $\varepsilon_0$  can represent  $\frac{\varepsilon}{2N}$ , which denotes the upper and lower levels of the IGs that have been generated uniformly.  $a_{ij}^-$  and  $a_{ij}^+$  represent the lower limit value and upper limit value of the information particle. For uniformly generated information particles, the distance between the lower limit value and the upper limit value is the same from the center. Each flexibly generated information particle is assigned a value based on the Gaussian probability distribution.

$$a_{ij}^- = \begin{cases} \min(a_{ij}(1 - \varepsilon_0), a_{ij}(1 + \varepsilon_0)) & \text{if } a_{ij} \neq 0 \\ -\varepsilon_0 & \text{if } a_{ij} = 0 \end{cases} \tag{15}$$

$$a_{ij}^+ = \begin{cases} \max(a_{ij}(1 - \varepsilon_0), a_{ij}(1 + \varepsilon_0)) & \text{if } a_{ij} \neq 0 \\ \varepsilon_0 & \text{if } a_{ij} = 0 \end{cases} \tag{16}$$

The flexible generation method [42] generates IGs based on data distribution in the output space using the Gaussian probability distribution. The size of each IG is not uniform.  $-\varepsilon$  and  $+\varepsilon$  are parameters that set the lower and upper bounds in the uniformly generated information particles, and their values are set based on the Gaussian probability distribution of the data.

$$a_{ij}^- = \begin{cases} \min(a_{ij}(1 - \varepsilon_{ij}^-), a_{ij}(1 + \varepsilon_{ij}^+)) & \text{if } a_{ij} \neq 0 \\ -\varepsilon_{ij}^- & \text{if } a_{ij} = 0 \end{cases} \tag{17}$$

$$a_{ij}^+ = \begin{cases} \max(a_{ij}(1 - \varepsilon_{ij}^-), a_{ij}(1 + \varepsilon_{ij}^+)) & \text{if } a_{ij} \neq 0 \\ \varepsilon_{ij}^+ & \text{if } a_{ij} = 0 \end{cases} \tag{18}$$

The method of generating IGs in the input space corresponding to each IG generated in the output space is to granulate the information around the cluster's centroid generated through clustering. For information granulation in the input space,  $x_k \in D(G(x_k, V_1, V_2, \dots, V_c, U))$  must be satisfied for as many data of  $X$  as possible. When the centroid of the cluster is granulated, the granulation of a specific level that assumes the value of  $[0, 1]$  for  $V_i$  is allowed.

$$V_{ij} = [v_{ij} - \varepsilon * range_j, v_{ij} + \varepsilon * range_j] \quad (19)$$

Here,  $i$  and  $j$  denote the number of clusters and the number of data, respectively. The cluster centroid is granulated at the same level for all data. Every coordinate of the cluster centroid is distributed symmetrically around  $v_{ij}$  and receives an equal effect by the given level of granulation. The higher the coverage, the higher the performance index (PI) [43].

Performance indices play an important role in evaluating model accuracy and clarity, and various methods have been developed to evaluate model performance. Common performance evaluation methods include Root Mean Square Error (RMSE) and Mean Absolute Percentage Error (MAPE). RMSE calculates the average of the squares by subtracting the model prediction value from the actual prediction value and then squaring the value to evaluate the performance. MAPE evaluates the performance by subtracting the model prediction value from the actual output value and dividing it by the model prediction value. This performance evaluation method is mainly used when the output value of the model is a numerical value. However, in the case of a granular model composed of information granules, since the model output value is an information granule rather than a numerical value, it is difficult to evaluate the model using a general performance evaluation method. To solve this problem, research on scalability and specificity has been actively conducted as a performance evaluation method for granular models. As the performance index has a higher value, it is a meaningful information granule, and a granular model with excellent performance can be designed. The PI is a non-increasing function of coverage. If the coverage is too high, it may not be allowed. Thus, the coverage can be re-assigned by setting a specific upper limit to generate effective IGs.

In order to generate reasonable information granules, two requirements are performed by the performance measure of coverage and specificity of information granules.

The coverage [43] indicates whether the target data are included in the formed information granules. In other words, it expresses how much the target total data are accumulated within the range of information granules and the degree of accumulation. The more data accumulated in the information granule, the higher the scalability value. It can prove the legitimacy of the information granule, so it can be a better model in relation to the modeling.

Specificity [43] indicates how specific and semantically explainable each information granule is. In other words, information granules should be created as detailed as possible, and each information granule should have an explanatory meaning. When the information granule is in the form of context, the narrower the interval between the upper and lower bounds, the higher the specificity.

The general GM generated IGs through cluster centroid and showed a limitation that processed every IG similarly by assigning the same coverage value for every variable. In this study, the coverage of the IGs generated in the output space and the number of IGs in the input space are re-assigning to generate meaningful IGs, which improves GM's prediction performance [43,44]. Figure 5 shows the process of generating rational IGs by re-assigning the variables of IGs generated in the output space. As shown in Figure 5, the information granule in the form of context has a lower bound and an upper bound. The middle vertex of the triangle is the model value.  $a_1$  is the lower bound of the model and  $a_2$  is the upper bound of the model. For  $a_1$  and  $a_2$ ,  $-$  and  $+$  are the ranges in which to optimize the lower and upper bounds to produce reasonable particles of information. Here, there are upper and lower limits. After random ranges are specified to the upper limits, the upper and lower limits that generate the satisfactory values for the coverage and specificity of IGs are searched using the optimization algorithm GA.

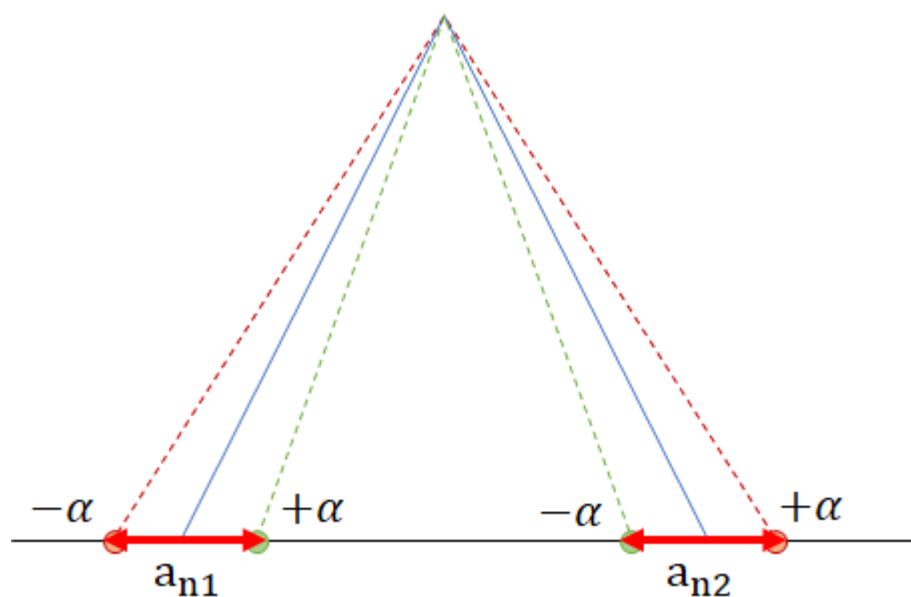


**Figure 5.** Variable assignment process of IGs generated in the output space for the generation of rational IGs.

### 3.2. Fuzzy-Based Granular Model and CGK-Based Fuzzy Granular Model of the Aggregated Structure Based on Rational IGs

In a hierarchical structure, the CGK-based fuzzy granular model of the aggregated structure uses the linear regression, neural network, and radial basis function neural network, which are generally used as prediction models as sub-models. Moreover, it also uses the CGK-based fuzzy granular model as the upper model. When the original numerical data are input to the sub-model, the output becomes a type 1 IG. When type 1 IG that combines the output calculated in the sub-model is input to the upper model, type 2 IG is generated through context-based GK clustering. The higher the number of types, the higher the level of abstraction; thus, it can represent a more meaningful IG that is verbally explainable.

The CGK-based fuzzy granular model of the aggregated structure generates IGs of the context shape in the output space and IGs of geometric shape in the input space. In this study, the IGs of the context shape generated in the output space of the CGK-based fuzzy granular model of the aggregated structure is optimally assigned through the GA [45,46] based on biological genetics. GA sets the number of generations, cross-operation ratio, and mutation ratio and optimizes by creating a new group using genetic operators. It calculates the goodness of fit to confirm whether the new group has the optimal solution. The goodness of fit is evaluated using the PI obtained through training and validation data after the generation is created. The goodness of fit can quantitatively indicate how much the generated solution is fit for solving the problem. The sequence of GA is as follows. The initial chromosome is generated by using the upper and lower limits of the context to be optimized. The goodness of fit of each chromosome is calculated through the PI. The current chromosome becomes a parent chromosome, and from these, the offspring chromosome is generated through crossover and mutation operations. After calculating the goodness of fit of the generated child chromosomes, the above process is stopped if it is a satisfactory value; otherwise, the child chromosomes are generated again, and the above process is repeated. Figure 6 shows the flowchart of the genetic algorithm. The lower and upper limits of the context are set as candidate solutions, the fitness computation of each chromosome is calculated, and the result is repeated until satisfactory.

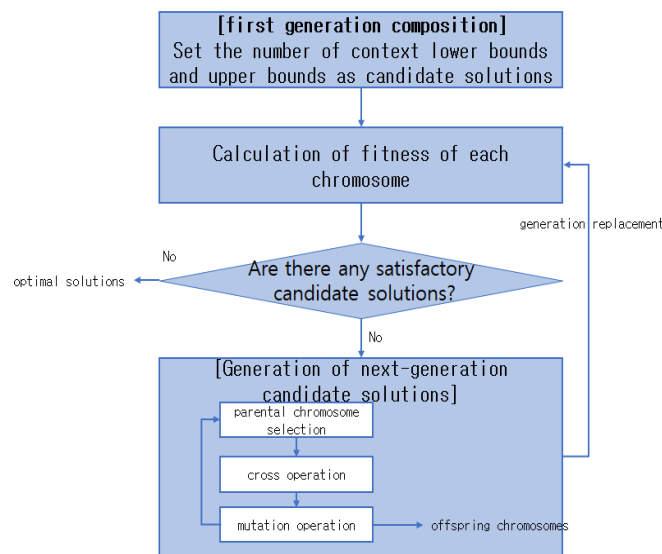


Figure 6. Flowchart of GA process.

The IGs of the optimally assigned output space, i.e., the IGs of the optimal context shape, are updated in the CGK-based GM to modify the spacing between contexts in the output space. In addition, IGs of the geometric shape are generated from the input space connected with each modified context to produce the optimal IGs in the input space and output space. Figure 7 shows the structure of the optimized CGK-based fuzzy granular model. Figure 8 shows the structure of the optimized CGK-based fuzzy granular model of the aggregated structure. This figure shows that IGs of the context shape are generated through the context-based GK clustering. Here, contexts are updated by optimizing the upper and lower limits of the context using GA, and through this, the optimized IGs of the geometric shape are generated in the input space. Figure 7 shows the structure of the optimized CGK-based fuzzy granular model. If you look at the output space in the figure, you can see a black context and a red context. Here, the black context is the existing context and the red context is the context optimized using GA.

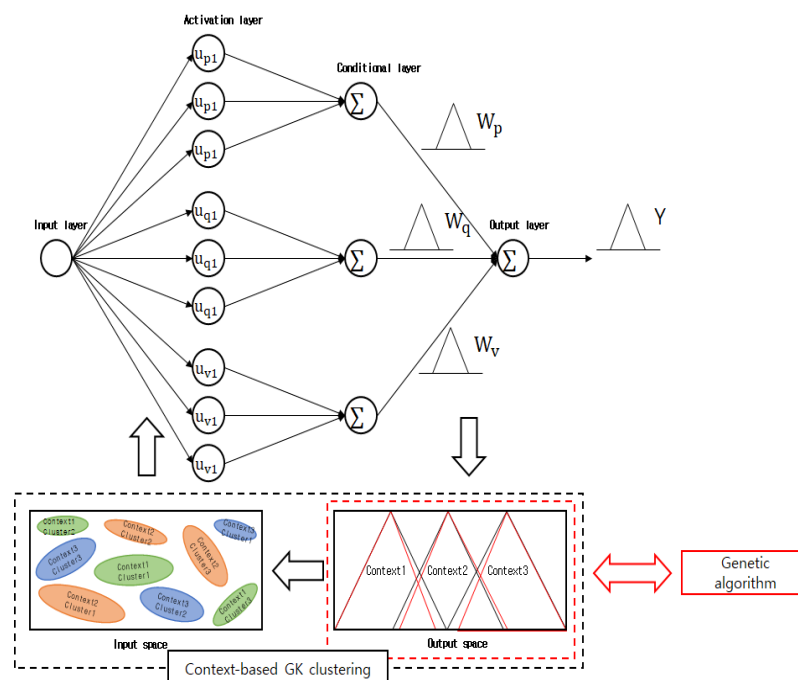


Figure 7. Structure of the optimized CGK-based fuzzy granular model.

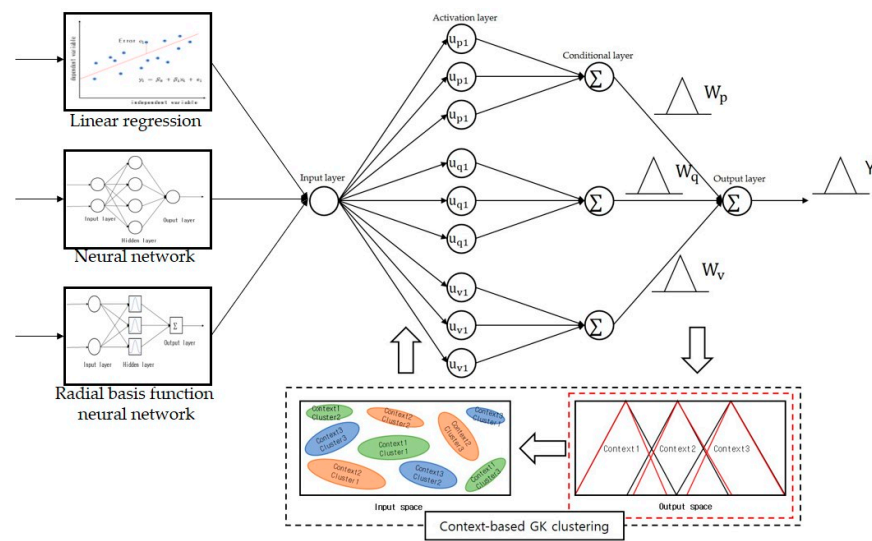


Figure 8. Structure of the optimized CGK-based fuzzy granular model of the aggregated structure.

#### 4. Experiments and Result Analysis

Experiments were conducted using the concrete compressive strength database [47] and Boston House Prices database [48], which are used in the prediction area to validate the optimized CGK-based fuzzy granular and the optimized CGK-based fuzzy granular models of the aggregated structure using GA proposed in this study. Considering the convenience for the analysis of experiment results, the proposed two fuzzy granular models are indicated by Optimal CGK-GM (Optimal Context-based Gustafson Kessel-Granular Model) and Optimal AGM (Optimal Aggregated Granular Model).

##### 4.1. Databases

The concrete compressive strength database, collected by the National Tsing Hua University in Taiwan, consists of 9 variables and 1030 instances. The input variables are cement, lime, fly ash, fine aggregates, blast furnace slag, coarse aggregates, water, and superplasticizer. The output variable is concrete compressive strength. The Boston House Prices database, which is a collection of information about the housing prices in Boston, consists of 14 variables and 506 instances. Input variables are per capita crime rate by town (CRIM), the proportion of residential land zone for lots over 25,000 sq. ft. (ZN), the proportion of non-retail business acres per town (INDUS), Charles River dummy variable (CHAS), nitric oxides concentration per 10 ppm (NOX), the average number of rooms per dwelling (RM), the proportion of owner-occupied units built before 1940 (AGE), weighted distances to five Boston employment centers (DIS), index of accessibility to radial highways (RAD), full-value property tax rate per \$10,000 (TAX), the pupil-teacher ratio by town (PTRATIO), the proportion of blacks by town (B), and % lower status of the population (LSTAT). The output variable is the median value of owner-occupied homes (MEDV).

##### 4.2. Experiment Method and Result Analysis

This study evaluates the prediction performance through the PI method, which is a performance evaluation method that is suitable for the IG and fuzzy granular model, instead of the generally used performance evaluation methods. As shown in Equation (20), the PI is expressed by the multiplication of coverage ( $\epsilon$ ), which is the coverage of IG, and specificity ( $\epsilon$ ), which is the specificity of IG. A value closer to 1 indicates higher performance. The experiment method is as follows. Each benchmarking database was divided into 50% for training and 50% for validation, and the PI was normalized to a value between 0 and 1. Experiments were conducted as the numbers of context (P) and cluster (C) of the CGK-GM, AGM, and the proposed Optimal CGK-GM and Optimal AGM were increased from 2 to 6. The fuzzy factor was fixed to 2. Furthermore, the two methods of generating contexts in

the output space, i.e., uniform and flexible generation methods, were compared. The GA used for context optimization was experimented with using the number of generations to 540, the cross-operation ratio of 0.97, and the mutation rate of 0.01.

$$\text{Performance index} = \text{coverage}(\varepsilon) \cdot \text{specificity}(\varepsilon) \quad (20)$$

The following shows the result of the concrete compressive strength prediction experiment. Table 1 shows the prediction performance of the CGK-based fuzzy granular model that generated contexts uniformly. Table 2 shows the prediction performance of the CGK-based fuzzy granular model that generated contexts flexibly. Tables 1 and 2 show that the higher the context, the higher the performance. The highest performance with a PI of 0.470 was achieved when the uniform generation method, six contexts, and four clusters were used. Figure 9 shows the output of the CGK-based fuzzy granular model and the real output. Figure 10 shows the PI of the CGK-based fuzzy granular model for the testing data. In Figure 9, the  $x$ -axis shows the number of concrete compressive strength, and the  $y$ -axis shows the concrete compressive strength. The solid black line indicates the real concrete compressive strength, whereas the red dotted line indicates the output of the CGK-based fuzzy granular model. In Figure 10, the  $x$ -axis shows the number of clusters generated in the input space, the  $y$ -axis shows the number of contexts generated in the output space, and the  $z$ -axis shows the PI for the validation data. Experiments were performed on the Windows 10 operating system, and the software used is MATLAB 2018a.

**Table 1.** Prediction performance CGK-based fuzzy granular model that generated contexts uniformly.

P	C					
	2	3	4	5	6	
2	0	0	0	0	0	
3	0.0204	0.0204	0.0204	0.02050	0.0206	
4	0.3328	0.3315	0.3308	0.3295	0.3315	
5	0.4409	0.4379	0.4350	0.4350	0.4300	
6	0.4618	0.4629	0.4700	0.4618	0.4606	

**Table 2.** Prediction performance CGK-based fuzzy granular model that generated contexts flexibly.

P	C					
	2	3	4	5	6	
2	0	0	0	0	0	
3	0.0295	0.0241	0.0282	0.0259	0.0233	
4	0.3060	0.3070	0.3084	0.3070	0.3052	
5	0.4182	0.4254	0.4183	0.4178	0.4162	
6	0.4662	0.4640	0.4569	0.4466	0.4449	

Tables 3 and 4 summarize the prediction performance of the CGK-based fuzzy granular model of the aggregated structure. Table 3 shows the result of the method that uniformly generated contexts, whereas Table 4 shows the effect of using the method that flexibly generates contexts. Based on the result of this table, the method of generating contexts uniformly was used, and the highest performance with a PI of 0.5208 was achieved when the number of contexts was six, and the number of clusters was 4.

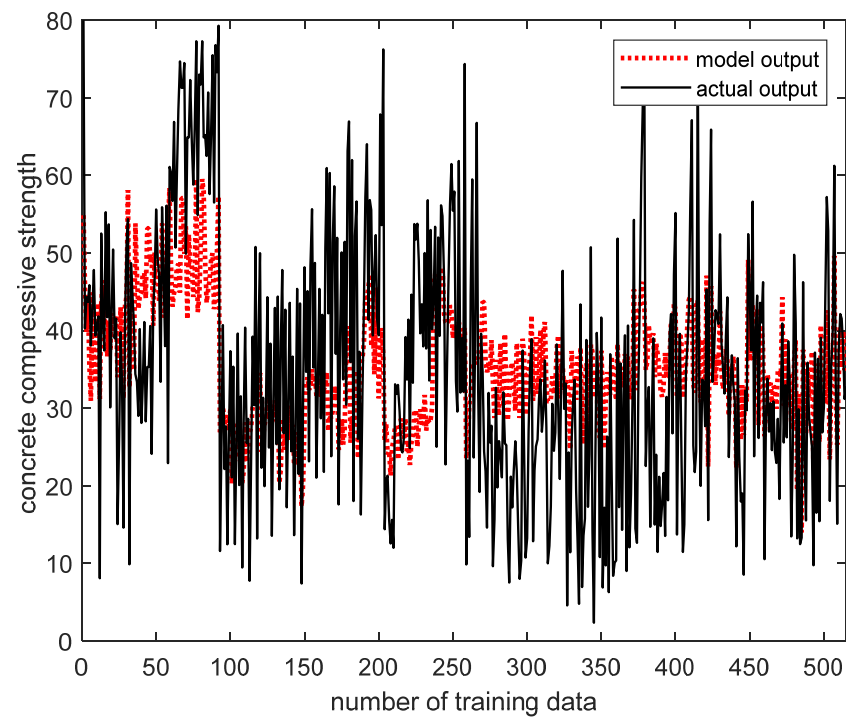


**Figure 9.** Comparison of the output of the CGK-based fuzzy granular model and real output (uniform generation of contexts, number of contexts = 6, number of clusters = 4).

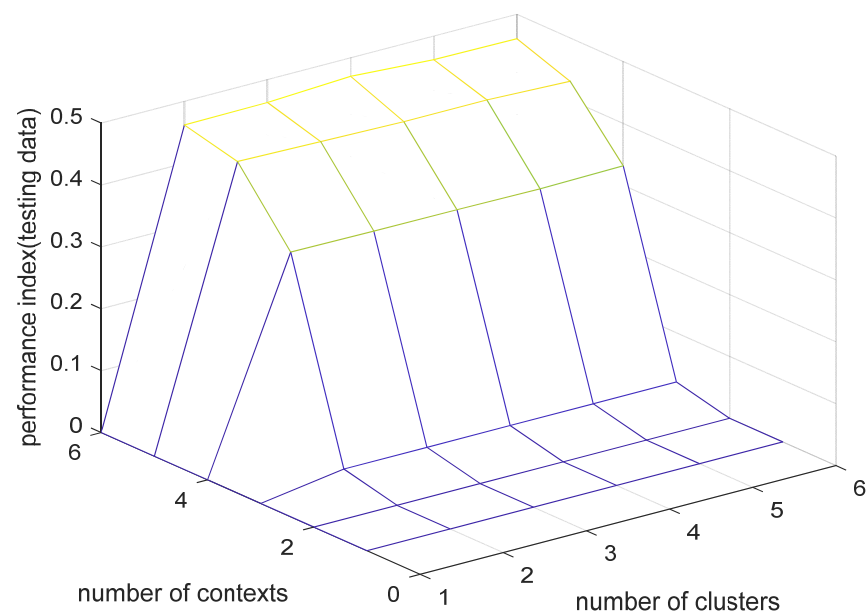


**Figure 10.** Performance index of the CGK-based fuzzy granular model for testing data (uniform generation of contexts, number of contexts = 6, number of clusters = 4).

Figure 11 shows the output of the CGK-based fuzzy granular model of the aggregated structure and the real output. Figure 12 shows the PI of the CGK-based fuzzy granular mode for validation data.

**Table 3.** Prediction performance CGK-based fuzzy granular model of the aggregated structure that generated contexts uniformly.

P	C					
	2	3	4	5	6	
2	0	0	0	0	0	
3	0.0201	0.0204	0.0203	0.0202	0.0203	
4	0.3194	0.3221	0.3302	0.3315	0.3295	
5	0.4548	0.4587	0.4548	0.4488	0.4637	
6	0.5125	0.5149	0.5208	0.5184	0.5196	

**Table 4.** Prediction performance CGK-based fuzzy granular model of the aggregated structure that generated contexts flexibly.

P	C					
	2	3	4	5	6	
2	0	0	0	0	0	
3	0.0481	0.0437	0.0446	0.0391	0.0451	
4	0.3071	0.3023	0.3136	0.3187	0.3129	
5	0.4344	0.4348	0.4380	0.4471	0.4418	
6	0.4884	0.4981	0.4921	0.5074	0.5028	

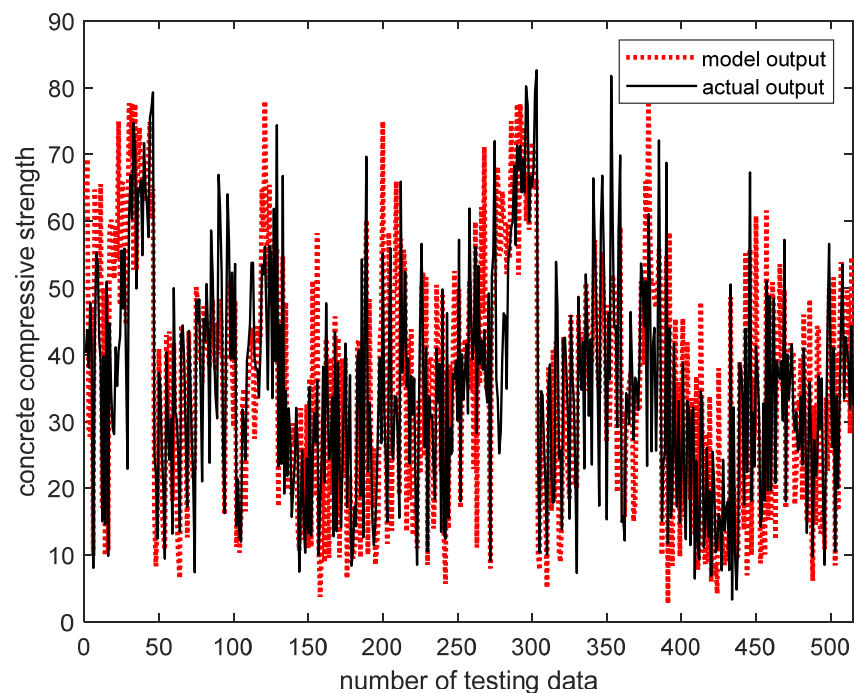


**Figure 11.** Comparison between the output of the CGK-based fuzzy granular model of the aggregated structure and the real output (uniform generation of contexts, number of contexts = 6, number of clusters = 4).

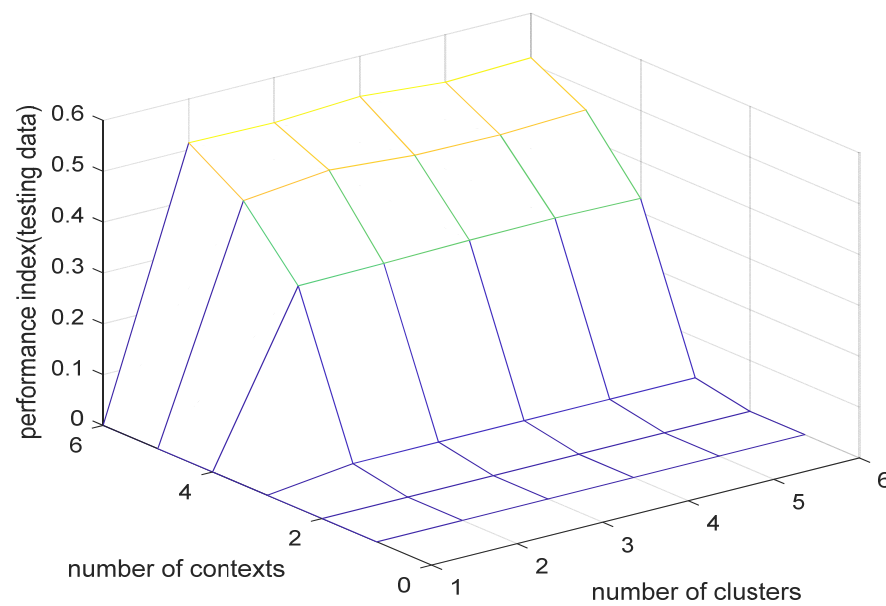


**Figure 12.** Performance index of the CGK-based fuzzy granular model of the aggregated structure for testing data (uniform generation of contexts, number of contexts = 6, number of clusters = 4).

Table 5 summarizes the prediction performance of the optimized CGK-based fuzzy granular model that generated contexts uniformly. Table 6 summarizes the prediction performance of the optimized CGK-based fuzzy granular model of the aggregated structure that generated contexts uniformly. Table 7 shows how the contexts in the output space of the optimized CGK-based fuzzy granular model were optimized from the existing shape. Table 8 shows how the contexts in the output space of the optimized CGK-based fuzzy granular model of the aggregated structure were optimized from the current shape. Here,  $p_{13}$  shows the upper limit of the first context and  $p_{21}$  shows the lower limit of the second context. Because the upper and lower limits of each context were set to the optimal values, the PIs of 0.4781 and 0.5386 were higher than the prediction performance of the conventional CGK-based fuzzy granular model and the CGK-based fuzzy granular model of the aggregated structure. Figure 13 compares the output of the optimized CGK-based fuzzy granular model and the real output. Figure 14 shows the PI of the optimized CGK-based fuzzy granular model. Figure 15 compares the output of the optimized CGK-based fuzzy granular model of the aggregated structure and the real value. Figure 16 shows the PI of the aggregated structure’s optimized CGK-based fuzzy granular model. These figures show the prediction of the optimized fuzzy granular model was closer to the real output than that of the conventional fuzzy granular model.

**Table 5.** Prediction performance of the optimized CGK-based fuzzy granular model.

P	C					
	2	3	4	5	6	
6	0.4497	0.4663	0.4781	0.4628	0.4687	

**Table 6.** Prediction performance of the optimized CGK-based fuzzy granular model with the aggregated structure.

P	C					
	2	3	4	5	6	
6	0.5168	0.5241	0.5143	0.5252	0.5386	

**Table 7.** Updated values after context optimization of the optimized CGK-based fuzzy granular model.

	$p_{13}$	$p_{21}$	$p_{23}$	$p_{31}$	$p_{33}$	$p_{41}$	$p_{43}$	$p_{51}$	$p_{53}$	$p_{61}$
Existing	17.8	2.3	33.3	17.8	48.9	33.3	64.4	48.9	79.9	64.4
Optimal	17.7	1.6	33.2	18.2	48.2	64	64	49.9	80.6	65.1

**Table 8.** Updated value after context optimization of the optimized CGK-based fuzzy granular model of the aggregated structure.

	$p_{13}$	$p_{21}$	$p_{23}$	$p_{31}$	$p_{33}$	$p_{41}$	$p_{43}$	$p_{51}$	$p_{53}$	$p_{61}$
Existing	17.8	2.3	33.3	17.8	48.9	33.3	64.4	48.9	79.9	64.4
Optimal	17.4	3.3	33.2	18.5	47.9	34	64.5	49.6	78.9	65.1

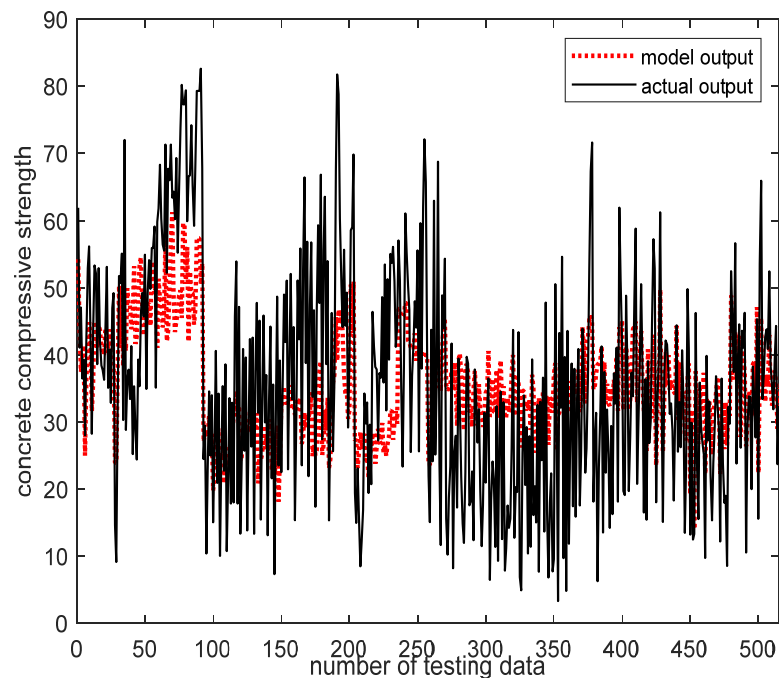


**Figure 13.** Comparison between the output of the optimized CGK-based fuzzy granular model and the real output.

Table 9 summarizes the results of the concrete compressive strength prediction experiment. The tables show the PI was high when the contexts were generated uniformly in every model. The validation PI of the CGK-based fuzzy granular model was 0.470 when six contexts and four clusters were used. The validation PI of the CGK-based fuzzy granular model of the aggregated structure was 0.5208 when six contexts and four clusters were used. The PIs of the optimized CGK-based fuzzy granular model and the optimized CGK-based fuzzy granular model of the aggregated structure proposed in this study were 0.4781 and 0.5386, respectively, when six contexts and six clusters were used. Therefore, these results confirmed that the proposed models show higher performance than the conventional fuzzy granular model.

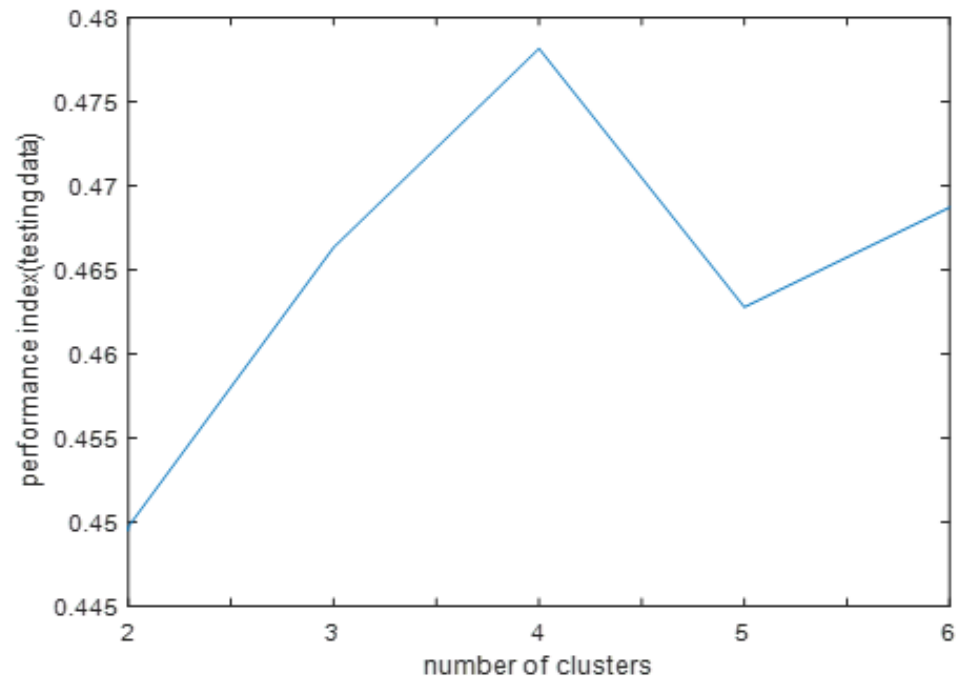


Figure 14. PI of the optimized CGK-based fuzzy granular model.

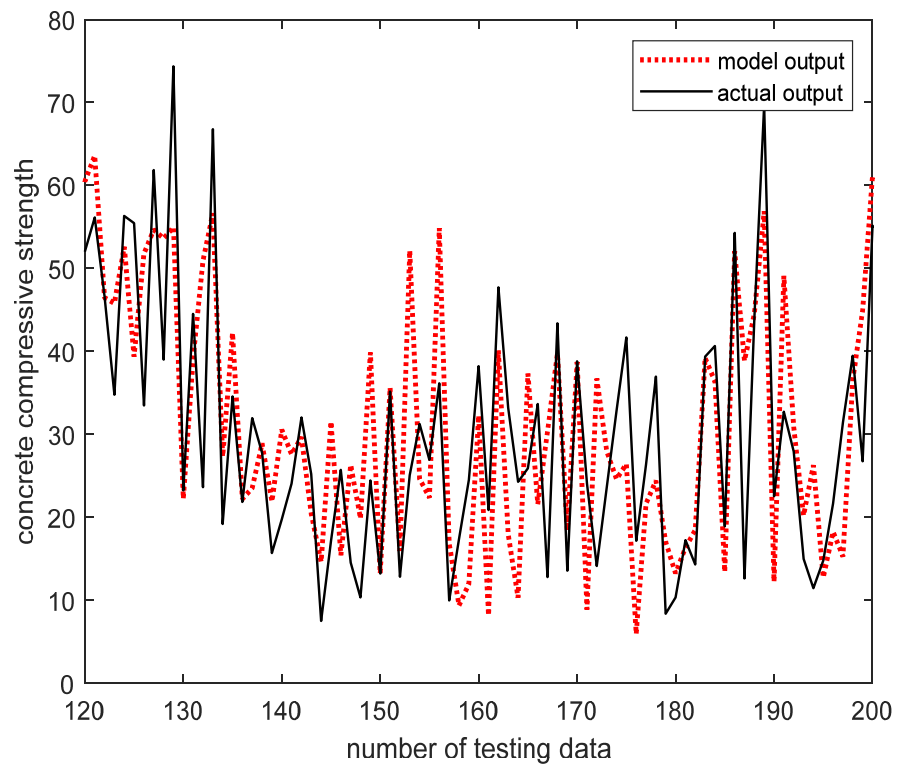
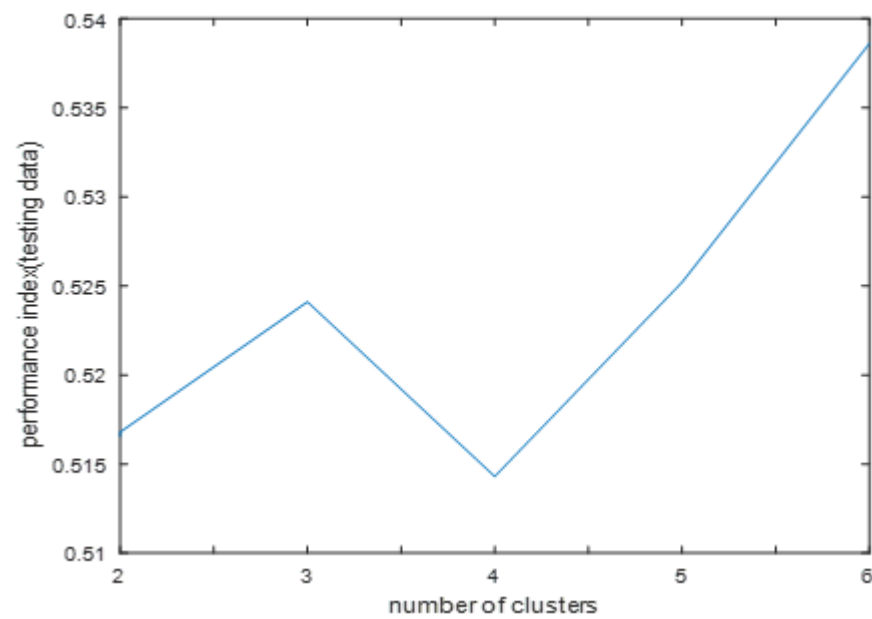


Figure 15. Comparison of the output of the optimized CGK-based fuzzy granular model of the aggregated structure and the real output.



**Figure 16.** Performance index of the optimized CGK-based fuzzy granular model of the aggregated structure.

**Table 9.** Result of the concrete compressive strength prediction experiment.

Model Types	IG Type	Num. of Contexts	Num. of Clusters	Training PI	Testing PI
CGK-GM	Uniform	6	4	0.4743	0.4700
A-CGK-GM	Uniform	6	4	0.5287	0.5208
Optimal CGK-GM	Uniform	6	6	0.4793	0.4781
Optimal A-CGK-GM	Uniform	6	6	0.5367	0.5386

Table 10 shows the result of the Boston House Prices prediction experiment. As shown in the table, the validation PI of the CGK-based fuzzy granular model was 0.5502 when the contexts were generated uniformly, and six contexts and five clusters were used. The PI of the CGK-based fuzzy granular model of the aggregated structure was 0.5870 when the contexts were generated flexibly, and six contexts and three clusters were used. The PI of the optimized CGK-based fuzzy granular model proposed was 0.5733 when the contexts were generated uniformly, and six contexts and five clusters were used. The optimized CGK-based fuzzy granular model of the aggregated structure showed the highest prediction performance with a validation PI of 0.6069 when contexts were generated flexibly, and six contexts and six clusters were used.

**Table 10.** Result of Boston House Prices prediction experiment.

Model Types	IG Type	Num. of Contexts	Num. of Clusters	Training PI	Testing PI
CGK-GM	Uniform	6	5	0.5476	0.5502
A-CGK-GM	Flexible	6	3	0.5287	0.5870
Optimal CGK-GM	Uniform	6	5	0.5698	0.5733
Optimal A-CGK-GM	Flexible	6	6	0.6100	0.6069

The results of experiments using two benchmarking databases for prediction confirmed that the optimized fuzzy granular models proposed showed higher prediction performance than the conventional CGK-based fuzzy granular model and the CGK-based fuzzy granular model of the aggregated structure. The prediction performance improved when the IGs were optimized through the GA. Furthermore, the performance of the context generation method changed according to the characteristics of the database.

## 5. Conclusions

In this paper, we proposed the optimized fuzzy-based granular model based on a hierarchical structure and optimal information granule allocation. Conventional fuzzy clustering generates clusters by calculating the distance between the center of the cluster and the data using the Euclidean distance. However, there is a problem in that the performance decreases when the data points have geometric characteristics. To improve this problem, GK clustering is used. GK clustering uses Mahalanobis distance to calculate the distance between the center of the cluster and the data to generate a geometrical cluster. On the basis of GK clustering, we proposed context-based GK (CGK) clustering, which generates the contexts in the output space and estimates the clusters each context. The advantages of the proposed CGK-based granular model can be summarized as follows:

Firstly, it is possible to automatically generate the explainable and meaningful fuzzy if-then rules that can be expressed linguistically by generating information granules in the input space and output space from numerical input and output data. Next, it is effective to process numerical input data points with specific geometric features. Since the output of the CGK-based granular model can be presented by the fuzzy number, it is possible to express the prediction result linguistically. Finally, we improved the performance by designing the CGK-based granular model with the aggregate structure that combines the linear regression model, neural network with multilayer, and radial basis function neural network.

In the future, based on the rational information granule generation principle, we plan to conduct the studies on generating various types of information granules and optimally allocating the information granules created in the input space and output space. In addition, we plan to design information granules that combine not only aggregated structures but also other types of hierarchical structures and predictive models.

**Author Contributions:** Conceptualization, C.-U.Y. and K.-C.K.; Methodology, C.-U.Y. and K.-C.K.; Software, C.-U.Y. and K.-C.K.; Validation, K.-C.K.; Formal Analysis, C.-U.Y. and K.-C.K.; Investigation, C.-U.Y. and K.-C.K.; Resources, K.-C.K.; Data Curation, C.-U.Y.; Writing-Original Draft Preparation, C.-U.Y.; Writing-Review and Editing, C.-U.Y. and K.-C.K.; Visualization, C.-U.Y.; Supervision, K.-C.K.; Project Administration, K.-C.K.; Funding Acquisition, K.-C.K. All authors have read and agreed to the published version of the manuscript.

**Funding:** This study was supported by research fund from Chosun University, 2022.

**Institutional Review Board Statement:** Not applicable.

**Informed Consent Statement:** Not applicable.

**Data Availability Statement:** Links to the databases used in this paper are provided as references.

**Conflicts of Interest:** The authors declare no conflict of interest.

## References

1. Zadeh, L.A. Fuzzy sets. *Arch. Wayback Mach. Inf. Control.* **2015**, *8*, 338–353. [[CrossRef](#)]
2. Couso, I.; Bustince, H. From fuzzy sets to interval-valued and atanassov intuitionistic fuzzy sets: A unified view of different axiomatic measures. *IEEE Trans. Fuzzy Syst.* **2018**, *27*, 362–371. [[CrossRef](#)]
3. Xie, T.; Gong, Z. A hesitant soft fuzzy rough set and its applications. *IEEE Access* **2019**, *7*, 167766–167783. [[CrossRef](#)]
4. Cazarez, R.L.U.; Diaz, N.G.; Equigua, L.S. Multi-layer adaptive fuzzy inference system for predicting student performance in online higher education. *IEEE Lat. Am. Trans.* **2021**, *19*, 98–106. [[CrossRef](#)]

5. Yeom, C.U.; Kwak, K.C. Performance comparison of ANFIS models by input space partitioning methods. *Symmetry* **2018**, *10*, 12. [\[CrossRef\]](#)
6. Ishak, K.E.H.K.; Ayoub, M.A. Predicting the efficiency of the oil removal from surfactant and polymer produced water by using liquid-liquid hydrocyclone comparison of prediction abilities between response surface methodology. *IEEE Access* **2019**, *7*, 179605–179619. [\[CrossRef\]](#)
7. An, J.; Fu, L.; Chen, W.; Zhen, J. A novel fuzzy-based convolutional neural network method to traffic flow prediction with uncertain traffic accident information. *IEEE Access* **2019**, *7*, 20708–20722. [\[CrossRef\]](#)
8. Yeom, C.U.; Kwak, K.C. Adaptive neuro-fuzzy inference system predictor with an incremental tree structure based on a context-based fuzzy clustering approach. *Appl. Sci.* **2020**, *10*, 23. [\[CrossRef\]](#)
9. Pedrycz, W.; Vasilakos, A.V. Linguistic models and linguistic modeling. *IEEE Trans. Syst. Man Cybern. Part B* **1999**, *29*, 745–757. [\[CrossRef\]](#)
10. Bargiela, A.; Pedrycz, W. *Granular Computing an Introduction*; Kluwer Academic Publishers: Norwell, MA, USA, 2003.
11. Zhu, X.; Pedrycz, W.; Li, Z. Granular models and granular outliers. *IEEE Trans. Fuzzy Syst.* **2018**, *26*, 3835–3846. [\[CrossRef\]](#)
12. Hmouz, R.A.; Pedrycz, W.; Balamash, A.S.; Morfeq, A. Hierarchical system modeling. *IEEE Trans. Fuzzy Syst.* **2017**, *26*, 258–269. [\[CrossRef\]](#)
13. Liu, Y.; Zhao, J.; Wang, W.; Pedrycz, W. Prediction intervals for granular data streams based on evolving type-2 fuzzy granular neural network dynamic ensemble. *IEEE Trans. Fuzzy Syst.* **2020**, *29*, 874–888. [\[CrossRef\]](#)
14. Pedrycz, W.; Kwak, K.C. Linguistic models as a framework of user-centric system modeling. *IEEE Trans. Syst. Man Cybern. Part A Syst. Hum.* **2006**, *6*, 727–745. [\[CrossRef\]](#)
15. Wang, S.; Pedrycz, W. Robust granular optimization a structured approach for optimization under integrated uncertainty. *IEEE Trans. Fuzzy Syst.* **2014**, *23*, 1372–1386. [\[CrossRef\]](#)
16. Zhu, X.; Pedrycz, W.; Li, Z. A development of granular input space in system modeling. *IEEE Trans. Cybern.* **2019**, *51*, 1639–1650. [\[CrossRef\]](#)
17. Truong, H.Q.; Ngo, L.T.; Pedrycz, W. Advanced fuzzy possibilistic C-means clustering based on granular computing. In Proceedings of the 2016 IEEE International Conference on Systems, Man, and Cybernetics, Budapest, Hungary, 9–12 October 2016.
18. Zuo, H.; Zhang, G.; Pedrycz, W.; Behbood, V.; Lu, J. Granular fuzzy regression domain adaptation in Takagi-Sugeno fuzzy models. *IEEE Trans. Fuzzy Syst.* **2017**, *26*, 847–858. [\[CrossRef\]](#)
19. Hu, X.; Pedrycz, W.; Wang, X. Granular fuzzy rule-based models a study in a comprehensive evaluation and construction of fuzzy models. *IEEE Trans. Fuzzy Syst.* **2016**, *25*, 1342–1355. [\[CrossRef\]](#)
20. Zhao, J.; Han, Z.; Pedrycz, W.; Wang, W. Granular model of long-term prediction for energy system in steel industry. *IEEE Trans. Cybern.* **2015**, *46*, 388–400. [\[CrossRef\]](#)
21. Zhou, Q.; Guo, S.; Xu, L.; Guo, X.; Williams, H.; Xu, H.; Yan, F. Global optimization of the hydraulic-electromagnetic energy-harvesting shock absorber for road vehicles with human-knowledge-integrated particle swarm optimization scheme. *IEEE/ASME Trans. Mechatron.* **2021**, *26*, 1225–1235. [\[CrossRef\]](#)
22. Kramer, M.; Bertram, T. Improving local trajectory optimization by enhanced initialization and global guidance. *IEEE Access* **2020**, *10*, 29633–29645. [\[CrossRef\]](#)
23. Holland, J. *Adaptation in Natural and Artificial Systems*; University of Michigan Press: Ann Arbor, MI, USA, 1975; ISBN 978-0-262-58111-0.
24. Kennedy, J.; Eberhart, R. Particle swarm optimization. *Proc. IEEE Int. Conf. Neural Netw.* **1995**, *4*, 1942–1948.
25. Peng, C.; Wu, X.; Yuan, W.; Zhang, X.; Zhang, Y. MGRFE: Multilayer recursive feature elimination based on an embedded genetic algorithm for cancer classification. *IEEE/ACM Trans. Comput. Biol. Bioinform.* **2019**, *18*, 621–632. [\[CrossRef\]](#) [\[PubMed\]](#)
26. Huanca, D.H.; Pareja, L.A.G. Chu and beasley genetic algorithm to solve the transmission network expansion planning problem considering active power losses. *IEEE Lat. Am. Trans.* **2021**, *19*, 1967–1975. [\[CrossRef\]](#)
27. Rojas, M.G.; Olivera, A.C.; Andrea, J. A memetic cellular genetic algorithm for cancer data microarray feature selection. *IEEE Lat. Am. Trans.* **2020**, *18*, 1874–1883. [\[CrossRef\]](#)
28. Souza, M.G.; Vallejo, E.E.; Estrada, K. Detecting clustered independent rare variant associations using genetic algorithms. *IEEE/ACM Trans. Comput. Biol. Bioinform.* **2019**, *18*, 932–939. [\[CrossRef\]](#)
29. Song, W.; Huang, C. Mining high utility itemsets using bio-inspired algorithms: A diverse optimal value framework. *IEEE Access* **2018**, *6*, 19568–19582. [\[CrossRef\]](#)
30. Zhao, Q.; Li, C. Two-stage multi-swarm particle swarm optimizer for unconstrained and constrained global optimization. *IEEE Access* **2020**, *8*, 124905–124927. [\[CrossRef\]](#)
31. Alonso, A.M.D.S.; Junior, B.R.P.; Brandao, D.I. Optimized exploitation of ancillary services: Compensation of reactive, unbalance and harmonic currents based on particle swarm optimization. *IEEE Lat. Am. Trans.* **2021**, *19*, 314–325. [\[CrossRef\]](#)
32. Li, P.; Liu, X.; Chen, H.; Li, B.; Ma, T.; Jiang, W. Optimization of three-dimensional magnetic field in vacuum Interrupter using particle swarm optimization algorithm. *IEEE Trans. Appl. Supercond.* **2021**, *31*, 5000804. [\[CrossRef\]](#)
33. Ibrahim, A.W.; Shafik, M.B.; Ding, M.; Sarhan, M.A.; Fang, Z.; Alareqi, A.G.; Almoqri, T.; Rassas, A.M.A. PV maximum power-point tracking using modified particle swarm optimization under partial shading conditions. *Chin. J. Electr. Eng.* **2020**, *6*, 106–121. [\[CrossRef\]](#)

34. Jia, X.; Lu, G. A hybrid taguchi binary particle swarm optimization for antenna designs. *IEEE Antennas Wirel. Propag. Lett.* **2019**, *18*, 1581–1585. [[CrossRef](#)]
35. Mi, Y.; Shi, Y.; Li, J.; Liu, W.; Yan, M. Fuzzy-based concept learning method: Exploting data with fuzzy conceptual clustering. *IEEE Trans. Cybern.* **2020**, *52*, 582–593. [[CrossRef](#)] [[PubMed](#)]
36. Gustafuson, D.E.; Kessel, W.C. Fuzzy clustering with a fuzzy covariance matrix. In Proceedings of the 1978 IEEE Conference on Decision and Control Including the 17th Symposium on Adaptive Processes, San Diego, CA, USA, 10–12 January 1979.
37. Freedman, D.A. *Statistical Models: Theory and Practice*; Cambridge University: Cambridge, UK, 2009.
38. Siegelmann, H.T.; Sontag, E.D. Turing computability with neural nets. *Appl. Math. Lett.* **1991**, *4*, 77–80. [[CrossRef](#)]
39. Broomhead, D.S.; Lowe, D. Multivariable functional interpolation and adaptive networks. *Complex Syst.* **1988**, *2*, 321–355.
40. Wang, L.; Han, Z.; Pedrycz, W.; Zhao, J. A granular computing-based hybrid hierarchical method for construction of long-term prediction intervals for gaseous system of steel industry. *IEEE Access* **2020**, *8*, 63538–63550. [[CrossRef](#)]
41. Pedrycz, W.; Hmouz, R.A.; Balamash, A.S.; Morfeq, A. Hierarchical granular clustering an emergence of information granules of higher type and higher order. *IEEE Trans. Fuzzy Syst.* **2015**, *23*, 2270–2283. [[CrossRef](#)]
42. Yeom, C.U.; Kwak, K.C. A design of CGK-based granular model using hierarchical structure. *Appl. Sci.* **2022**, *12*, 3154. [[CrossRef](#)]
43. Zhu, X.; Pedrycz, W.; Li, Z. A design of granular Takagi-Sugeno fuzzy model through the synergy of fuzzy subspace clustering and optimal allocation of information granularity. *IEEE Trans. Fuzzy Syst.* **2018**, *26*, 2499–2509. [[CrossRef](#)]
44. Lu, W.; Pedrycz, W.; Yang, J.; Liu, X. Granular fuzzy modeling guided through the synergy of granulating output space and clustering input subspaces. *IEEE Trans. Cybern.* **2019**, *51*, 2625–2638. [[CrossRef](#)]
45. Aamir, M.; Tu, S.; Tolouei, M.R.; Giasin, K.; Vafadar, A. Optimization and modeling of process parameters in multi-hole simultaneous drilling using taguchi method and fuzzy logic approach. *Materials* **2020**, *13*, 680. [[CrossRef](#)]
46. Katoch, S.; Chauhan, S.; Kumar, V. A review on genetic algorithm: Past present, and future. *Multimed. Tools Appl.* **2021**, *80*, 8091–8126. [[CrossRef](#)] [[PubMed](#)]
47. Available online: <http://lib.stat.cmu.edu/datasets/boston> (accessed on 13 July 2022).
48. UCI Machine Learning Repository, Concrete Compressive Strength Data Set. Available online: <https://archive.ics.uci.edu/ml/datasets/Concrete+Compressive+Strength> (accessed on 13 July 2022).